PHYSICAL REVIEW B **88**, 214409 (2013)

Phase-space Berry phases in chiral magnets: Dzyaloshinskii-Moriya interaction and the charge of skyrmions

Frank Freimuth,[1,*] Robert Bamler,[2] Yuriy Mokrousov,[1] and Achim Rosch[2]

[1]*Peter Grünberg Institut and Institute for Advanced Simulation, Forschungszentrum Jülich and JARA, 52425 Jülich, Germany*

[2]*Institute for Theoretical Physics, Universität zu Köln, D-50937 Köln, Germany*

(Received 5 September 2013; revised manuscript received 22 November 2013; published 11 December 2013)

The semiclassical motion of electrons in phase space $\mathbf{x} = (\mathbf{R},\mathbf{k})$ is influenced by Berry phases described by a six-component vector potential $\mathbf{A} = (\mathbf{A}^{\mathrm{R}},\mathbf{A}^{\mathrm{k}})$. In chiral magnets, Dzyaloshinskii-Moriya (DM) interactions induce slowly varying magnetic textures (helices and skyrmion lattices) for which all components of $\mathbf{A}$ are important, inducing effectively a curvature in mixed position and momentum space. We show that for smooth textures and weak spin-orbit coupling, phase-space Berry curvatures determine the DM interactions and give important contributions to the charge. Using *ab initio* methods, we calculate the strength of DM interactions in MnSi in good agreement with experiment and estimate the charge of skyrmions.

DOI: 10.1103/PhysRevB.88.214409 PACS number(s): 75.10.Lp, 03.65.Vf, 71.15.Mb, 71.20.Lp

I. INTRODUCTION

In chiral magnets without inversion symmetry, spin-orbit interaction (SOI) effects described by Dzyaloshinskii-Moriya (DM) interactions[1,2] induce the formation of magnetic textures. For smooth textures and cubic systems such as MnSi, the leading DM contribution to the free-energy density is given by the term $D\hat{\mathbf{n}}\cdot(\nabla\times\hat{\mathbf{n}})$, where $\hat{\mathbf{n}}$ is the direction of the magnetization. This term describes that energy can be gained when the magnetic structure twists. In small magnetic fields, these interactions (in combination with thermal fluctuations) can stabilize lattices of topologically quantized magnetic whirls, so called skyrmions.[3,4] Skyrmions couple due to their topological winding extremely efficiently to electric currents resulting in ultralow critical currents for the motion of skyrmions.[5–7]

In this paper, we argue that Berry phases in phase space provide not only a natural framework to understand the physical properties of skyrmions and other magnetic textures, but also generate DM interactions and act therefore as the main driving force inducing magnetic textures in chiral magnets. We focus on Berry curvatures in mixed position and momentum space which lead both to DM interactions and also to an electric charge of skyrmions. Thereby, we naturally link skyrmions in chiral magnets to skyrmions in quantum Hall systems with filling close to $\nu = 1$, which are characterized by a quantized electric charge.[8–12]

Berry phases are quantum mechanical phases picked up by a quantum system when the wave function changes adiabatically.[13–15] They can strongly affect the semiclassical motion of electrons. For each electronic band n, the effects of smoothly varying magnetic textures can efficiently be described by a six-component vector potential $\mathbf{A}_n = (\mathbf{A}_n^{\mathrm{R}},\mathbf{A}_n^{\mathrm{k}})$, with

$$A_{n,j}(\mathbf{x}) = \langle \mathbf{x},n|i\frac{\partial}{\partial x_j}|\mathbf{x},n\rangle, \quad j = 1,\ldots,6 \tag{1}$$

where $\mathbf{x} = (\mathbf{R},\mathbf{k})$ is the position in phase space and $|\mathbf{x},n\rangle = |\hat{\mathbf{n}}(\mathbf{R}),\mathbf{k},n\rangle$ is the Bloch function, which depends not only on lattice momentum $\hbar\mathbf{k}$, but also on the orientation $\hat{\mathbf{n}}(\mathbf{R})$ of the magnetization. Here, we use the letter $\mathbf{R}$ to denote smooth variations on length scales much larger than the lattice spacing.

Two aspects of Berry phase physics have been well studied in the context of chiral magnets. First, Berry phases in momentum space, described by the $\mathbf{k}$ dependence of $\mathbf{A}_n^{\mathrm{k}}(\mathbf{x})$, give rise to the anomalous Hall effect,[16] which dominates the Hall response for a wide range of temperatures and fields in materials such as MnSi.[17] Powerful *ab initio* methods have been developed to calculate the anomalous Hall effect quantitatively.[18–22] Second, real-space Berry phases give rise to the so-called topological Hall effect. For weak SOI, each skyrmion contributes due to their topology one flux quantum of an emergent magnetic flux,[23] arising from the effective magnetic field $B_{n,i}^{\mathrm{R}} = \frac{\hbar}{e}\epsilon_{ijk}\partial_{R_j}A_{n,k}^{\mathrm{R}} \approx \pm\frac{\hbar}{4e}\epsilon_{ijk}\hat{\mathbf{n}}\cdot(\partial_{R_j}\hat{\mathbf{n}}\times\partial_{R_k}\hat{\mathbf{n}})$ with positive (negative) sign for majority (minority) band n, respectively. This real-space emergent magnetic field acts similar to the "real" magnetic field and has been observed in MnSi (Refs. 3 and 23) and other materials (see, e.g., Refs. 24 and 25) as an extra contribution to the Hall signal. The same effect is also responsible for the efficient coupling of skyrmions to electric currents.[5–7]

Much less studied are systems with Berry phases in phase space, where the $\mathbf{R}$ dependence of $\mathbf{A}_n^{\mathrm{k}}(\mathbf{x})$ and the $\mathbf{k}$ dependence of $\mathbf{A}_n^{\mathrm{R}}(\mathbf{x})$ become important. It has been argued that such a situation arises in smoothly deformed crystals[14] or in the presence of spatially varying external magnetic fields. Also, in antiferromagnets with slowly varying spin texture the mixed Berry phase was suggested to crucially influence the adiabatic dynamics of electrons.[26] Some of us[27] have recently pointed out that DM interactions arise from certain Berry phases. Here, we will provide a purely semiclassical derivation of the Berry phase contribution to the DM interaction showing that DM interactions can be viewed as a phase-space Berry phase effect. By the same mechanism, magnetic skyrmions also obtain a charge. In general, chiral magnets and their magnetic phases turn out to be ideal model systems to study phase-space Berry phases due to their smoothly varying magnetic textures driven by DM interactions.

II. PHASE-SPACE BERRY PHASES

As has been shown by Niu *et al.*[14,28] phase-space Berry phases effectively lead to a curvature of phase space described

by the antisymmetric 6×6 Berry-curvature tensor[28]

$$\Omega_{n,ij} = \frac{\partial A_{n,j}}{\partial x_i} - \frac{\partial A_{n,i}}{\partial x_j} = \begin{pmatrix} \Omega_n^{\mathrm{RR}} & \Omega_n^{\mathrm{Rk}} \\ \Omega_n^{\mathrm{kR}} & \Omega_n^{\mathrm{kk}} \end{pmatrix}_{ij}. \tag{2}$$

Here, $\Omega_{n,ij}^{\mathrm{RR}} = \frac{e}{\hbar}\epsilon_{ijk}B_{n,k}^{\mathrm{R}}$ describes real-space Berry phases while $\Omega_{n,ij}^{\mathrm{kk}}$ encodes the momentum-space Berry phases also discussed above. The 3×3 matrix $\Omega_{n,ij}^{\mathrm{Rk}} dR_i dk_j$ is the Berry phase which is picked up when an electron moves along a loop in the phase-space plane spanned by the coordinates R_i and k_j.

The Berry phases influence the semiclassical description of the system in three points. First, the combination of smooth variations in both position and momentum space leads to a shift of the semiclassical energy levels[14] $\epsilon_n(\mathbf{x}) = \epsilon_n^{(0)}(\mathbf{x}) + \delta\epsilon_n(\mathbf{x})$ where $\epsilon_n^{(0)}(\mathbf{x}) = \langle \mathbf{x},n|H(\mathbf{x})|\mathbf{x},n\rangle$ and

$$\delta\epsilon_n(\mathbf{x}) = -\mathrm{Im}\left[\frac{\partial\langle \mathbf{x},n|}{\partial R_i}\left[\epsilon_n^{(0)}(\mathbf{x}) - H(\mathbf{x})\right]\frac{\partial|\mathbf{x},n\rangle}{\partial k_i}\right]. \tag{3}$$

Second, the Berry phases modify the semiclassical equations of motion,[14] which read as $(\Omega_n - J)\dot{\mathbf{x}} = \frac{\partial\epsilon_n}{\partial\mathbf{x}}$ where $J = \left(\begin{smallmatrix} 0 & \mathbb{1} \\ -\mathbb{1} & 0 \end{smallmatrix}\right)$. Third, the curvature of phase space leads in semiclassical approximation to a modified density of states in phase space[28,29]

$$\begin{aligned} W_n(\mathbf{x}) &= \sqrt{\det(\Omega_n - J)} \\ &= \frac{\epsilon_{ijklrs}}{48}(\Omega_n - J)_{ij}(\Omega_n - J)_{kl}(\Omega_n - J)_{rs}. \end{aligned} \tag{4}$$

Only for this modified density of states the above semiclassical equations of motion satisfy the Liouville theorem. A derivation of Eq. (4) is given in Appendix B.

III. SEMICLASSICS FOR CHIRAL MAGNETS

While the Berry phase description has originally been developed for noninteracting systems, it can also be used to calculate ground-state properties in the presence of interactions using that, within density functional theory (DFT), the interacting system is mapped to a noninteracting one. In the following, we describe an *ab initio* method for the calculation of the DM interaction strength and the charge density in chiral magnets with weak SOI. The method is based on DFT calculations in the homogeneous (i.e., ferromagnetic) state. Berry phase effects coming from the inhomogeneous magnetic texture are then taken into account by means of a gradient expansion.

Within DFT, one can describe the ground state of a ferromagnetic many-particle system with magnetization $\mathbf{M}$ parallel to the unit vector $\hat{\mathbf{n}}$ by an effective single-particle Kohn-Sham Hamiltonian

$$H_{\hat{\mathbf{n}}} = \frac{\mathbf{p}^2}{2m} + V(\mathbf{r}) - \mathbf{M}\cdot\mathbf{B}(\mathbf{r}) - \frac{1}{2mc^2}\mathbf{M}\cdot[\mathbf{E}(\mathbf{r})\times\mathbf{p}], \tag{5}$$

parametrized by an effective potential $V(\mathbf{r})$, an exchange field $\mathbf{B}(\mathbf{r})$, and an electric field $\mathbf{E}(\mathbf{r})$. We use the letter $\mathbf{r}$ for variations on the atomic length scale. To obtain such a ferromagnetic state in a chiral magnet, one has to apply a small external field $\mathbf{B}^{\mathrm{ext}}$ in the direction of $\hat{\mathbf{n}}$ (implicitly included in $\mathbf{B}$) (see following). In the absence of SOI, V and $\mathbf{E}$ are independent of $\hat{\mathbf{n}}$, while $\mathbf{B} \parallel \hat{\mathbf{n}}$.

A. DM interaction

Starting from the eigenstates $|\hat{\mathbf{n}},\mathbf{k},n\rangle$ of the *uniform* Hamiltonian (5) for fixed $\hat{\mathbf{n}}$, we can obtain the change of the free-energy density $\delta F^{(1)}(\mathbf{R})$ to leading order in an adiabatic approximation. We assume that $\hat{\mathbf{n}}(\mathbf{R})$ slowly varies in space and use Eqs. (3) and (4) with $|\mathbf{x},n\rangle = |\hat{\mathbf{n}}(\mathbf{R}),\mathbf{k},n\rangle$ to obtain

$$\begin{aligned} \delta F^{(1)}(\mathbf{R}) = \sum_n \int \frac{d^3k}{(2\pi)^3}\Bigg[& f_{\mathbf{k}n}\delta\epsilon_n(\mathbf{x}) \\ & + \frac{1}{\beta}\ln(1 + e^{-\beta(\epsilon_{\mathbf{k}n}-\mu)})\Omega_{n,ii}^{\mathrm{Rk}}(\mathbf{x})\Bigg]. \end{aligned} \tag{6}$$

Note that to leading order all contributions arise from mixed position- and momentum-space Berry curvatures (see following). They contribute only when both inversion symmetry is broken and SOI is present.

To calculate $\delta\epsilon_n(\mathbf{x})$ and the Berry curvature $\Omega_{n,ii}^{\mathrm{Rk}}(\mathbf{x})$ directly, we use that the change of an eigenstate $|n\rangle$ upon changing a parameter λ of H is given by $\partial_\lambda|n\rangle = \sum_{m\neq n}\frac{|m\rangle}{E_n - E_m}\langle m|\frac{\partial H}{\partial\lambda}|n\rangle$ and therefore the Berry curvature and the energy shift read as

$$\Omega_{n,ij} = -2\sum_{m\neq n}\mathrm{Im}\frac{\langle \mathbf{x},n|\frac{\partial H}{\partial x_i}|\mathbf{x},m\rangle\langle \mathbf{x},m|\frac{\partial H}{\partial x_j}|\mathbf{x},n\rangle}{\left[\epsilon_n^{(0)}(\mathbf{x}) - \epsilon_m^{(0)}(\mathbf{x})\right]^2}, \tag{7}$$

$$\delta\epsilon_n = -\sum_{m\neq n}\mathrm{Im}\frac{\langle \mathbf{x},n|\frac{\partial H}{\partial R_i}|\mathbf{x},m\rangle\langle \mathbf{x},m|\frac{\partial H}{\partial k_i}|\mathbf{x},n\rangle}{\epsilon_n^{(0)}(\mathbf{x}) - \epsilon_m^{(0)}(\mathbf{x})}. \tag{8}$$

The derivative with respect to crystal momentum is identified with the velocity $\mathbf{v}$, while the derivative with respect to position arises from the $\mathbf{R}$ dependence of $\hat{\mathbf{n}}$:

$$\frac{1}{\hbar}\frac{\partial H}{\partial k_i} = v_i, \quad \frac{\partial H}{\partial R_i} = \frac{\partial H}{\partial\hat{\mathbf{n}}}\cdot\frac{\partial\hat{\mathbf{n}}}{\partial R_i} = \mathbf{T}(\mathbf{r})\cdot\left(\hat{\mathbf{n}}\times\frac{\partial\hat{\mathbf{n}}}{\partial R_i}\right), \tag{9}$$

where $\mathbf{T}(\mathbf{r}) = \hat{\mathbf{n}}\times\frac{\partial H}{\partial\hat{\mathbf{n}}}$ is the torque operator. Thus, we arrive at

$$\delta F^{(1)}(\mathbf{R}) = D_{ij}\hat{\mathbf{e}}_i\cdot\left(\hat{\mathbf{n}}\times\frac{\partial\hat{\mathbf{n}}}{\partial R_j}\right), \tag{10}$$

with

$$\begin{aligned} D_{ij} &= \sum_n\int\frac{d^3k}{(2\pi)^3}\left[f_{\mathbf{k}n}A_{\mathbf{k}nij} + \frac{\ln[1+e^{-\beta(\epsilon_{\mathbf{k}n}-\mu)}]B_{\mathbf{k}nij}}{\beta}\right], \\ A_{\mathbf{k}nij} &= \hbar\sum_{m\neq n}\mathrm{Im}\left[\frac{\langle \mathbf{k}n|T_i|\mathbf{k}m\rangle\langle \mathbf{k}m|v_j(\mathbf{k})|\mathbf{k}n\rangle}{\epsilon_{\mathbf{k}m} - \epsilon_{\mathbf{k}n}}\right], \\ B_{\mathbf{k}nij} &= -2\hbar\sum_{m\neq n}\mathrm{Im}\left[\frac{\langle \mathbf{k}n|T_i|\mathbf{k}m\rangle\langle \mathbf{k}m|v_j(\mathbf{k})|\mathbf{k}n\rangle}{(\epsilon_{\mathbf{k}m} - \epsilon_{\mathbf{k}n})^2}\right], \end{aligned} \tag{11}$$

where $A_{\mathbf{k}nij}$ describes the Berry energy (3), $\delta\epsilon_n = A_{\mathbf{k}ni'i}(\hat{\mathbf{n}}\times\frac{\partial\hat{\mathbf{n}}}{\partial R_i})_{i'}$, and $B_{\mathbf{k}nij}$ the Berry curvature $\Omega_{n,ij}^{\mathrm{Rk}} = B_{\mathbf{k}ni'j}(\hat{\mathbf{n}}\times\frac{\partial\hat{\mathbf{n}}}{\partial R_i})_{i'}$, respectively.

Equation (10) can directly be identified with the DM interaction[1,2] in the continuum limit. We have therefore shown that for smooth textures and weak SOI, the DM interaction arises from mixed momentum- and position-space Berry curvatures and the corresponding energy shifts obtained from the Kohn-Sham Hamiltonian. Our semiclassical derivation yields the same expression for D_{ij} as obtained from quantum mechanical perturbation theory.[27]

At $T = 0$, to linear order in $\nabla\hat{\mathbf{n}}$ and for weak SOI, the formula (10) is exact even for a fully interacting quantum system [provided the exact Kohn-Sham Hamiltonian is used in Eq. (5)]. To calculate changes of the ground-state energy to linear order, changes of H due to $\nabla\hat{\mathbf{n}}$ can be neglected (a manifestation of the magnetic force theorem[30]). Therefore, the only remaining source of errors is the external magnetic field $\boldsymbol{B}^{\text{ext}}$ needed to stabilize the ferromagnetic solution underlying Eq. (5). As this field can be chosen to be weak (second order in SOI strength), it does not affect the value of the DM interaction to leading order in SOI.

Aside from DM interactions, also the current-induced spin-orbit torque relies on broken inversion symmetry. Recently, it has been shown that the intrinsic contribution to this torque is related to the Berry curvature $B_{\mathbf{k}nij}$.[31]

B. Charge density

The change of charge density to first order in the gradients of the magnetization also arises from both the change of the density of states and the energy levels from phase-space curvatures. It is given by

$$\delta\rho^{(1)}(\mathbf{R}) = e\sum_n \int \frac{d^3k}{(2\pi)^3}\left[\frac{\partial f_{\mathbf{k}n}}{\partial\epsilon}\delta\epsilon_n(\mathbf{x}) - f_{\mathbf{k}n}\,\Omega^{\text{Rk}}_{nii}(\mathbf{x})\right], \tag{12}$$

where $e = -|e|$ is the electron charge. We obtain

$$\begin{aligned}\delta\rho^{(1)}(\mathbf{R}) &= e\,G_{ij}\hat{\mathbf{e}}_i\cdot\left(\hat{\mathbf{n}}\times\frac{\partial\hat{\mathbf{n}}}{\partial R_j}\right),\\ G_{ij} &= \int\frac{d^3k}{(2\pi)^3}\sum_n\left[\frac{\partial f_{\mathbf{k}n}}{\partial\epsilon_{\mathbf{k}n}}A_{\mathbf{k}nij} - f_{\mathbf{k}n}B_{\mathbf{k}nij}\right].\end{aligned} \tag{13}$$

In metals, extra charges are screened on the length scale set by the Thomas-Fermi screening length λ_{TF}, resulting in a strongly suppressed charge density $\rho_{\text{tot}} \approx -\lambda_{\text{TF}}^2\nabla^2(\delta\rho^{(1)})$. Since the metal screens extra charge by changing the occupation of the states on the Fermi surface, while the Fermi sea participates in the formation of $\delta\rho^{(1)}$, the calculation of the unscreened $\delta\rho^{(1)}$ is interesting to understand how many electrons are energetically redistributed between Fermi surface and Fermi sea due to the phase-space Berry phases.

The results of our semiclassical derivation can be reproduced by a gradient expansion of the Green's function similar to the technique used by Yang *et al.* in Ref. 32 for insulators (see Appendix C). While to leading order in $\nabla\hat{\mathbf{n}}$ the semiclassical formulas (3) and (4) are reproduced, higher orders give for metals rise to additional contributions to the density of states that are not captured by the higher-order terms of Eq. (4) as we have checked explicitly.

In insulators, the situation is different. Neither energy shifts [Eq. (3)] nor the term linear in Ω_n in Eq. (4) contribute to the total charge of a single skyrmion. The integral $\int\frac{dR_x dk_x}{2\pi}\Omega^{\text{Rk}}_{n,xx}$, for example, has to be quantized (first Chern number). As it evaluates to 0 for $y\to\infty$, it vanishes everywhere. All contributions to the charge arise from higher-order terms in the gradient expansion. As the charge has to be a topological invariant in an insulator, it can be calculated from an adiabatically deformed band structure where all occupied bands are completely flat and degenerate. In this limit, one can use standard arguments[33] to show that the total accumulated charge due to smooth variations in phase space, e.g., in two space dimensions, is given by the second Chern number

$$\begin{aligned}\delta Q^{(2)} &\equiv \int d^2R\,\delta\rho^{(2)}\\ &= -e\int\frac{d^2R\,d^2k}{(2\pi)^2}\frac{\epsilon_{ijkl}}{8}\text{Tr}[\Omega_{ij}\Omega_{kl}],\end{aligned} \tag{14}$$

where Ω is a matrix in the space of occupied bands. We refer to Appendix C 3 for the derivation of Eq. (14).

Therefore, either Abelian or non-Abelian winding numbers can occur. In cases when all non-Abelian winding numbers vanish, the right-hand side of Eq. (14) coincides with the integral over the term quadratic in Ω_n on the right-hand side of Eq. (4). For Abelian situations, $\delta Q^{(2)}$ can be expressed as a product of two simple real-space and momentum-space winding numbers (i.e., two first Chern numbers) $\delta Q^{(2)} = \sigma_{xy}\Phi_0$, where $\sigma_{xy} = \frac{e^2}{\hbar}\int\frac{d^2k}{(2\pi)^2}\Omega^{\text{kk}}_{xy}$ is the quantized Hall conductivity and $\Phi_0 = \frac{\hbar}{|e|}\int d^2R\,\Omega^{\text{RR}}_{xy}$ the quantized total flux arising from the real-space Berry phases. This can be shown by rewriting Eq. (14) as a surface integral and using, for example, that for $\mathbf{R}\to\infty$ both Ω^{RR} and Ω^{Rk} vanish (see Appendix C 4 for details).

IV. RESULTS

A. Qualitative dependency on the SO strength

In order to investigate first qualitatively how the accumulated charge in metals depends on the strength of SOI, we consider the simple two-dimensional two-band toy model

$$H = \epsilon_{\mathbf{k}} + [\mathbf{b}^{\text{ex}}(\mathbf{R}) + \mathbf{g}^{\text{so}}(\mathbf{k})]\cdot\boldsymbol{\sigma} = \epsilon_{\mathbf{k}} + \mathbf{n}(\mathbf{R},\mathbf{k})\cdot\boldsymbol{\sigma}, \tag{15}$$

where $\boldsymbol{\sigma}$ is the vector of Pauli matrices, $\mathbf{b}^{\text{ex}}(\mathbf{R})$ the exchange field arising from the magnetic texture, $\mathbf{g}^{\text{so}}(\mathbf{k})$ the SOI field, and $\mathbf{n} = \mathbf{b}^{\text{ex}} + \mathbf{g}^{\text{so}}$. From Eqs. (1)–(3), one finds

$$\Omega_{\pm,ij} = \mp\frac{1}{2}\hat{\mathbf{n}}\cdot\left(\frac{\partial}{\partial x_i}\hat{\mathbf{n}}\times\frac{\partial}{\partial x_j}\hat{\mathbf{n}}\right), \tag{16}$$

$$\delta\epsilon_+ = \delta\epsilon_- = |\mathbf{n}|\sum_{i=1}^{3}\Omega^{\text{Rk}}_{+,ii}, \tag{17}$$

where $\pm$ labels the minority and majority bands, respectively. To analyze the model (15) analytically, we consider the limit of weak SOI parameter λ_{so} with $|\mathbf{g}^{\text{so}}|/|\mathbf{b}^{\text{ex}}| \sim \lambda_{\text{so}}$. SOI also controls the size of skyrmions as their formation is driven by DM interactions. For skyrmion lattices in chiral magnets, the diameter of the skyrmions is proportional to $1/\lambda_{\text{so}}$ (Ref. 3). Expanding Eqs. (16) and (17) in λ_{so} shows that both $\delta\epsilon_\pm$ and *all* components of Ω are of order λ^2_{so}. This argument shows that the expansion in powers of Ω, which lead to Eq. (6), is valid for chiral magnets with weak SOI. Remarkably, all factors of λ_{so} cancel, when the total charge of a single skyrmion $\delta Q^{(1)} = \int\delta\rho^{(1)}\,d^2R$ is calculated using Eq. (12). Assuming that the exchange field $\mathbf{b}^{\text{ex}}$ is small compared to the Fermi

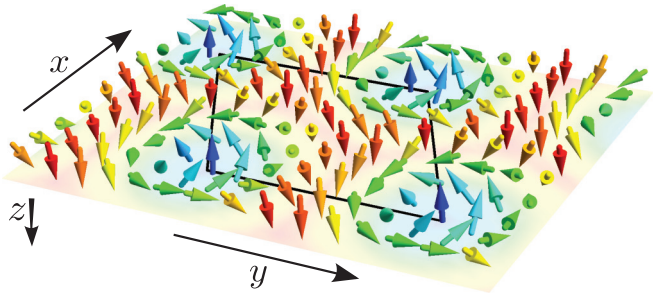

FIG. 1. (Color online) Illustration of the exchange field $\mathbf{b}^{\mathrm{ex}}(\mathbf{R})$ in a skyrmion lattice [Eq. (19)]. Arrows are colored according to their z component and spaced in an arbitrary distance much larger than the atomic lattice constant in MnSi. The black polygon encloses the magnetic unit cell. In the three-dimensional system, the magnetic texture is translationally invariant in the z direction.

energy, we find

$$D_{ij} \approx \frac{|\mathbf{b}^{\mathrm{ex}}|^2}{3} \int \frac{d^2k}{(2\pi)^2} \frac{\partial g_i^{\mathrm{so}}}{\partial k_j} f''(\epsilon_{\mathbf{k}}),$$
$$\delta Q^{(1)} \approx \frac{2}{3} e \int \frac{d^2R\, d^2k}{(2\pi)^2} |\mathbf{b}^{\mathrm{ex}}|^3\, \Omega^{\mathrm{Rk}}_{+,ii}\, f'''(\epsilon_{\mathbf{k}}). \tag{18}$$

To obtain a qualitative estimate, we assume $|\partial g^{\mathrm{so}}/\partial k| \sim \lambda_{\mathrm{so}} E_F a$ where E_F is the Fermi energy and a the lattice constant. According to neutron scattering experiments,[3,34] the skyrmion lattice in MnSi is well described by (see Fig. 1 for an illustration)

$$\mathbf{b}^{\mathrm{ex}}(\mathbf{R}) = B_0 \hat{\mathbf{z}} + B_1 \sum_{n=0}^{2} [(\hat{\mathbf{z}} \times \hat{\boldsymbol{\xi}}_n) \sin(q_0 \hat{\boldsymbol{\xi}}_n \cdot \mathbf{R}) + \hat{\mathbf{z}} \cos(q_0 \hat{\boldsymbol{\xi}}_n \cdot \mathbf{R})], \tag{19}$$

where $q_0 \approx 2\pi/190$ Å, $\hat{\mathbf{z}} = (0,0,1)$ is the unit vector parallel to a small magnetic field stabilizing the skyrmion lattice, and $\hat{\boldsymbol{\xi}}_n = [\cos(2\pi n/3), \sin(2\pi n/3), 0]$. From mean-field calculations,[34] $B_1/B_0 \approx -1.5$ is obtained. As q_0 is linear in λ_{so}, we set $q_0 = \lambda_{\mathrm{so}} 2\pi/a$. In this model, we obtain

$$D_{ij} \sim \lambda_{\mathrm{so}}\, \delta_{ij} \frac{E_F}{a} \frac{B_0^2}{E_F^2}, \quad \delta Q^{(1)} \sim e \frac{B_0^2}{E_F^2}. \tag{20}$$

As expected, the DM interaction is linear in SOI and quadratic in the magnetization. Interestingly, the skyrmion charge is *independent* of the SOI strength (when screening is ignored) but proportional to the square of the local magnetization. These main conclusions remain valid when we calculate the charge with *ab initio* methods using the real band structure of a complex material (see following).

B. Quantitative results for the DM interaction strength and the skyrmion charge in MnSi

Based on the electronic structure of MnSi obtained within the local density approximation (LDA), we compute D_{ij} and G_{ij} at $T = 0$ using Wannier functions[35,36] to reduce the computational burden (see Appendix A for computational details). Furthermore, we approximate V, $\mathbf{E}$, and $\mathbf{B}$ in Eq. (5) by their value for vanishing spin-orbit coupling. This allows us to perform the calculation at $\mathbf{B}^{\mathrm{ext}} = 0$ using that $\mathbf{B} \parallel \hat{\mathbf{n}}$. The torque is then simply given by $\mathbf{T} = \mathbf{M} \times \mathbf{B}$. For a left-handed crystal structure, we obtain $D_{ij} = -D\delta_{ij}$ with

$$D = -4.1 \text{ meV Å per eight-atom cell.} \tag{21}$$

An experimental value for D can be obtained from neutron scattering in the helical phase of MnSi because a finite D shifts the minimum of $E(q) = Dq + Jq^2$ from $q = 0$ to $-D/(2J)$ for a left-handed spiral. Using $J = 52$ meV Å^2 per eight-atom cell[37] and $q = 2\pi/190$ Å leads to an experimental value of $D = -3.43$ meV Å in good agreement with our result.

Next, we discuss the manifestations of phase-space Berry phases on the skyrmions in MnSi. As $G_{ij} \propto D_{ij} \propto \delta_{ij}$ by symmetry, $\delta F^{(1)}(\mathbf{R})$ and $\delta\rho^{(1)}(\mathbf{R})$ are proportional to each other and can therefore be shown in a single plot (see Fig. 2), where we used $\hat{\mathbf{n}}(\mathbf{R}) = \mathbf{b}^{\mathrm{ex}}/|\mathbf{b}^{\mathrm{ex}}|$ [with $\mathbf{b}^{\mathrm{ex}}$ from Eq. (19)]. Integrating $\delta F^{(1)}(\mathbf{R})$ over the magnetic unit cell, we obtain a free-energy reduction of 231 meV. Both charge density and free-energy density are maximal in the center of the skyrmion located at (0,0). Integrating $\delta\rho^{(1)}(\mathbf{R})$ over the magnetic unit cell, we obtain the charge of $0.246e$. However, $\delta\rho^{(1)}(\mathbf{R})$ is strongly

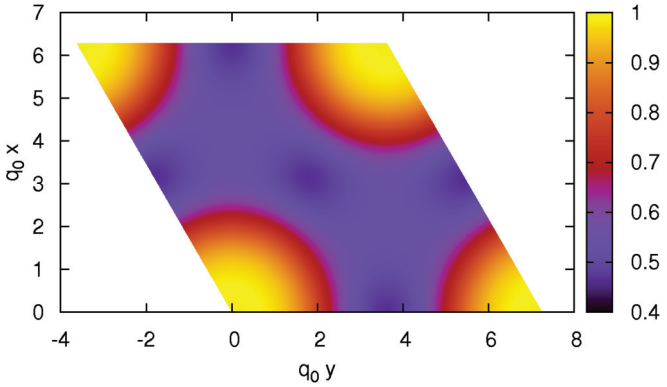

FIG. 2. (Color online) Normalized free-energy density $\delta F^{(1)}(\mathbf{R})/\delta F^{(1)}(0)$ and normalized charge density $\delta\rho^{(1)}(\mathbf{R})/\delta\rho^{(1)}(0)$ within the magnetic unit cell. The minimal free-energy density is given by $\delta F^{(1)}(0) = -0.0018$ meV/Å^3, the total free energy is reduced by 231 meV per skyrmion and layer. The maximal charge density amounts to $\delta\rho^{(1)}(0) = 1.95 \times 10^{-6} e$/Å^3, the total charge per skyrmion and layer is $0.246e$. The skyrmion center is located at the origin, as in Eq. (19) (cf. Fig. 1).

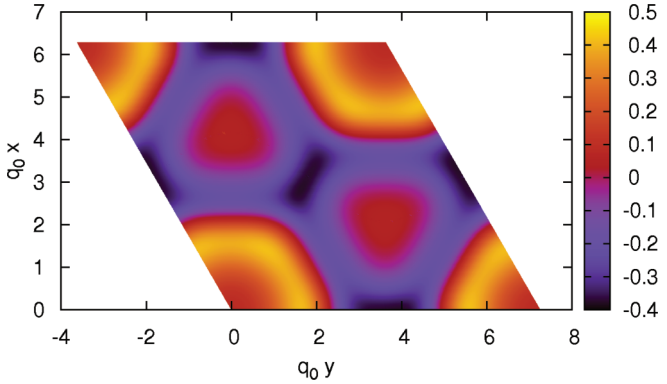

FIG. 3. (Color online) Screened charge density $\rho_{\mathrm{tot}}/[\delta\rho^{(1)}(0)\lambda_{\mathrm{TF}}^2 q_0^2]$ within the magnetic unit cell, with $\delta\rho^{(1)}(0)\lambda_{\mathrm{TF}}^2 q_0^2 = 1.07 \times 10^{-10} e$/Å^3.

screened due to the short $\lambda_{\rm TF} = \sqrt{\epsilon_0/(e^2 N_F)} \approx 0.224$ Å, where $N_F \approx 0.11/(\text{eV Å}^3)$ is the density of states at the Fermi level obtained in our LDA calculations. The resulting screened charge density varies between $\rho_{\rm tot}^{\rm max} \approx 4.5 \times 10^{-11} e/\text{Å}^3$ close to the core and $\rho_{\rm tot}^{\rm min} \approx -4.1 \times 10^{-11} e/\text{Å}^3$ between two skyrmions (see Fig. 3 for illustration).

V. CONCLUSIONS

Our analysis has shown that mixed real-space/momentum-space Berry phases are quantitatively important in materials such as MnSi. Energetically, they are the driving force for the formation of magnetic textures and lead to a redistribution of charge in the skyrmion phase which we calculated using *ab initio* methods. For the future, it will be interesting to investigate how the phase-space Berry curvature $\Omega^{\rm Rk}$ affects the Hall effect. As in MnSi, the contributions arising from the topological Hall effect, i.e., from $\Omega^{\rm RR}$, and the anomalous Hall effect due to $\Omega^{\rm kk}$, are of similar magnitude, we also expect substantial contributions from $\Omega^{\rm Rk}$.

ACKNOWLEDGMENTS

We thank S. Blügel, H. Geiges, C. Pfleiderer, M. Zirnbauer, and, especially, A. Altland for illuminating discussions. Financial support of the DFG (SFB TR 12, FOR 960), funding under the HGF-YIG programme VH-NG-513 and from Deutsche Telekom Stiftung (R.B.), and computing time on the supercomputers JUQUEEN and JUROPA at Jülich Supercomputing Center are gratefully acknowledged.

APPENDIX A: COMPUTATIONAL DETAILS OF THE *AB INITIO* CALCULATIONS

From the full-potential linearized augmented-plane-wave code FLEUR (Ref. 38), the electronic structure of MnSi was obtained within the local density approximation[39] to density functional theory. The atomic coordinates and lattice parameter ($a = 4.558$ Å) of the eight-atom unit cell of MnSi as given in Ref. 40, muffin-tin radii of $2.12a_0$ for both Mn and Si, and a plane-wave cutoff of $3.7a_0^{-1}$ were used in the calculations ($a_0 = 0.529\,177$ Å is Bohr's radius). The basis set was supplemented with local orbitals for the Mn $3s$ and $3p$ states. The unconstrained spin moment per formula unit is $0.94\mu_{\rm B}$ and thus larger than the measured spin moment by more than a factor of 2. We constrained the spin moment per formula unit to the value of $0.4\mu_{\rm B}$. From the relativistic first-principles Bloch functions of 100 bands given on an $8\times8\times8$ **k** mesh, we constructed 64 relativistic maximally localized Wannier functions using disentanglement within the WANNIER90 code.[41] The lowest 40 bands in the valence window are the 32 local orbitals plus 8 Mn $4s$ bands. These were skipped, i.e., the 100 bands from which the Wannier functions were disentangled are bands 41 to 140.

Based on Wannier interpolation,[42,43] we evaluated $D_{ij}(\hat{\mathbf{n}})$ for the 001, 111, and 110 directions $\hat{\mathbf{n}}$ of magnetization using a $512\times512\times512$ interpolation mesh. We find that to very good approximation

$$\mathbf{D}_j(\hat{\mathbf{n}}) = D_{ij}(\hat{\mathbf{n}})\hat{\mathbf{e}}_i = D\hat{\mathbf{n}} \times (\hat{\mathbf{n}} \times \hat{\mathbf{e}}_j), \tag{A1}$$

where $\hat{\mathbf{e}}_1 = \hat{\mathbf{x}}$, $\hat{\mathbf{e}}_2 = \hat{\mathbf{y}}$, and $\hat{\mathbf{e}}_3 = \hat{\mathbf{z}}$ are unit vectors of the Cartesian coordinate system and a single parameter $D = -7.69a_0/V$ meV describes the amplitude of DMI, with $V = a^3$ the volume of the unit cell. Equation (A1) neglects the anisotropy of $\mathbf{D}_j(\hat{\mathbf{n}})$, which is small according to our calculations.

Using Eq. (A1), we can express $\delta F^{(1)}(\mathbf{R})$ as follows:

$$\begin{aligned}\delta F^{(1)}(\mathbf{R}) &= \mathbf{D}_i(\hat{\mathbf{n}}) \cdot \left(\hat{\mathbf{n}} \times \frac{\partial \hat{\mathbf{n}}}{\partial R_i}\right) \\ &= D\hat{\mathbf{n}} \cdot [\nabla \times \hat{\mathbf{n}}].\end{aligned} \tag{A2}$$

In the skyrmion lattice in MnSi, only the derivatives $\partial_x \hat{\mathbf{n}}$ and $\partial_y \hat{\mathbf{n}}$ contribute and $\partial_z \hat{\mathbf{n}} = 0$. Thus, we have

$$\nabla \times \hat{\mathbf{n}} = \begin{pmatrix} -\sin\theta\, \frac{\partial\theta}{\partial y} \\ \sin\theta\, \frac{\partial\theta}{\partial x} \\ \cos\theta\sin\phi\, \frac{\partial\theta}{\partial x} + \sin\theta\cos\phi\, \frac{\partial\phi}{\partial x} - \\ \cos\theta\cos\phi\, \frac{\partial\theta}{\partial y} + \sin\theta\sin\phi\, \frac{\partial\phi}{\partial y} \end{pmatrix}, \tag{A3}$$

yielding an alternative expression for $\delta F^{(1)}(\mathbf{R})$ in terms of the azimuthal and polar angles of the exchange field and their derivatives:

$$\begin{aligned}\delta F^{(1)}(\mathbf{R}) &= D\Big[\sin\phi\frac{\partial\theta}{\partial x} - \cos\phi\frac{\partial\theta}{\partial y} \\ &\quad + \sin\theta\cos\theta\Big(\cos\phi\frac{\partial\phi}{\partial x} + \sin\phi\frac{\partial\phi}{\partial y}\Big)\Big] \\ &= Dq_0\mathcal{Q}(q_0x, q_0y),\end{aligned} \tag{A4}$$

where

$$\begin{aligned}\mathcal{Q}(q_0x, q_0y) = \Big[&\sin\phi\frac{\partial\theta}{\partial(q_0x)} - \cos\phi\frac{\partial\theta}{\partial(q_0y)} \\ &+ \sin\theta\cos\theta\Big(\cos\phi\frac{\partial\phi}{\partial(q_0x)} + \sin\phi\frac{\partial\phi}{\partial(q_0y)}\Big)\Big].\end{aligned} \tag{A5}$$

We define the free energy per skyrmion $\delta E^{(1)}$ as integral of $\delta F^{(1)}(\mathbf{R})$ over the magnetic unit cell, where we set the extension of the magnetic cell in the z direction equal to the lattice parameter a of the eight-atom unit cell of MnSi. We obtain

$$\begin{aligned}\delta E^{(1)} &= a\int \delta F^{(1)}(\mathbf{R})dx\,dy \\ &= \frac{aD}{q_0}\int d\,(q_0x)d\,(q_0y)\mathcal{Q}(q_0x, q_0y) \\ &= 39\frac{aD}{q_0} = -231\ \text{meV}.\end{aligned} \tag{A6}$$

Determining the tensor

$$t_{ij} = e\int \frac{d^3k}{(2\pi)^3}\sum_n f_{\mathbf{k}n}B_{\mathbf{k}nij} \tag{A7}$$

from Wannier interpolation, we get

$$t_{ij}(\hat{\mathbf{n}}) = t\hat{\mathbf{e}}_i \cdot [\hat{\mathbf{n}} \times (\hat{\mathbf{n}} \times \hat{\mathbf{e}}_j)], \tag{A8}$$

with $t = -0.091ea_0/V$, where small anisotropies of t_{ij} have been neglected. t_{ij} describes the intrinsic component of the SOI-mediated spin torque per volume to an applied electric

field in the homogeneous system.[31] One contribution to $\delta\rho^{(1)}(\mathbf{R})$ is given by

$$-t_{ij}\hat{\mathbf{e}}_i \cdot \left(\hat{\mathbf{n}} \times \frac{\partial \hat{\mathbf{n}}}{\partial R_j}\right). \tag{A9}$$

However, due to the additional Fermi surface term, the complete expression for $\delta\rho^{(1)}(\mathbf{R})$ is given by

$$\delta\rho^{(1)}(\mathbf{R}) = eG_{ij}\hat{\mathbf{e}}_i \cdot \left(\hat{\mathbf{n}} \times \frac{\partial \hat{\mathbf{n}}}{\partial R_j}\right), \tag{A10}$$

where according to our calculations

$$eG_{ij} = g\hat{\mathbf{e}}_i \cdot [\hat{\mathbf{n}} \times (\hat{\mathbf{n}} \times \hat{\mathbf{e}}_j)], \tag{A11}$$

with $g = 0.0082\frac{ea_0}{V}$, neglecting again the small anisotropies. Similar to rewriting the free-energy density above, we obtain

$$\delta\rho^{(1)}(\mathbf{R}) = g\hat{\mathbf{n}} \cdot [\nabla \times \hat{\mathbf{n}}] = gq_0\mathcal{Q}(q_0x, q_0y). \tag{A12}$$

We define the charge per skyrmion $\delta Q^{(1)}$ as integral of $\delta\rho^{(1)}(\mathbf{R})$ over the magnetic unit cell, where we set the extension of the magnetic cell in the z direction equal to the lattice parameter a of the eight-atom unit cell of MnSi. This yields

$$\begin{aligned}\delta Q^{(1)} &= a\int \delta\rho^{(1)}(\mathbf{R})dx\,dy \\ &= \frac{ag}{q_0}\int d\,(q_0x)d\,(q_0y)\mathcal{Q}(q_0x, q_0y) \\ &= 39\frac{ag}{q_0} = 0.246e.\end{aligned} \tag{A13}$$

APPENDIX B: COORDINATE INDEPENDENT FORMULATION OF THE PHASE-SPACE VOLUME

In this section, we review the derivation of the volume element [Eq. (4)] of the main text following mostly the review by Morrison[29] and rewrite some of our formulas using differential forms. This makes the derivation transparent and is manifestly independent of the chosen coordinate system.[44,45]

Consider a transformation from canonical coordinates X_i with standard Poisson brackets $\{f,g\} = \frac{\partial f}{\partial X_i}J_{ij}\frac{\partial g}{\partial X_j}$ to a new set of coordinates $x_i = x_i(\mathbf{X})$. The Poisson brackets of the (noncanonical) coordinates x_i are given by

$$\{x_i, x_j\} = \frac{\partial x_i}{\partial X_{i'}}J_{i'j'}\frac{\partial x_j}{\partial X_{j'}} = (\omega^{-1})_{ij}. \tag{B1}$$

The natural volume element of the $2d$-dimensional phase space is obtained from the Jacobi determinant $|\partial X_i/\partial x_j|$:

$$dV = \frac{d^{2d}X}{(2\pi)^d} = \left|\frac{\partial X_i}{\partial x_j}\right|\frac{d^{2d}x}{(2\pi)^d} = \sqrt{\det\omega}\,\frac{d^{2d}x}{(2\pi)^d}, \tag{B2}$$

where we used that $\det\omega = (|\partial x_i/\partial X_j|^2 \det J)^{-1} = |\partial X_i/\partial x_j|^2$ as $\det J = 1$ and $\det M^{-1} = 1/\det M$.

It is useful to rewrite Eq. (B2) using that the phase-space volume dV is independent of the coordinate system. In canonical coordinates, we define the 2-form $\hat{\omega}$ from the inverse of $J^{-1} = -J$ using

$$\hat{\omega} = \frac{1}{2}(J^{-1})_{ij}\,dX^i \wedge dX^j \tag{B3}$$

$$= \frac{1}{2}\frac{\partial X_{i'}}{\partial x_i}(J^{-1})_{i'j'}\frac{\partial X_{j'}}{\partial x_j}\,dx^i \wedge dx^j$$

$$= \frac{1}{2}\omega_{ij}\,dx^i \wedge dx^j, \tag{B4}$$

where we used the definition of ω from Eq. (B1). As in Eq. (B3), $\hat{\omega}$ is expressed in canonical coordinates, the phase-space volume is directly obtained from the d-fold wedge product $\hat{\omega}^d = \hat{\omega} \wedge \ldots \wedge \hat{\omega}$:

$$dV = \frac{\hat{\omega}^d}{d!(2\pi)^d}\,. \tag{B5}$$

While Eqs. (B2) and (B5) are equivalent, Eq. (B5) is much easier to handle due to the missing square root.

A remarkable aspect is the close relation of Poisson brackets, phase-space volume, Berry connections, and Chern classes. The semiclassical equations of motion for an electron in band n in the presence of phase-space Berry phases are given in the main text as

$$\dot{x}_i = [(\Omega_n - J)^{-1}]_{ij}\,\frac{\partial\epsilon_n}{\partial x_j} \equiv \{x_i, \epsilon_n\}, \tag{B6}$$

where the Poisson brackets are defined by Eq. (B1) with $\omega = \Omega_n - J$. From Eq. (B4) follows

$$\hat{\omega} = \tfrac{1}{2}[(J^{-1})_{ij} + \Omega_{ij}]\,dx^i \wedge dx^j = \hat{\omega}_0 + \hat{\Omega}, \tag{B7}$$

where $\hat{\omega}_0 = \frac{1}{2}(J^{-1})_{ij}\,dx^i \wedge dx^j$ is the "canonical" 2-form which obtains a correction from the Abelian Berry curvature

$$\hat{\Omega} = d\hat{A} = \tfrac{1}{2}\Omega_{ij}\,dx^i \wedge dx^j, \tag{B8}$$

where $\hat{A} = A_i\,dx_i$ and we have omitted all band indices. From Eqs. (B5) and (B7), one obtains Eq. (4) of the main text.

The Berry curvature directly gives the first Chern form

$$\hat{c}_1 = \frac{\hat{\Omega}}{2\pi}. \tag{B9}$$

Integrals of the wedge product of m such Chern forms, $\int \hat{c}_1^m = \int \hat{c}_1 \wedge \ldots \wedge \hat{c}_1$, over compact $2m$-dimensional manifolds without boundary define Chern numbers which are quantized to integers.[46] Such wedge products directly show up when expanding dV in powers of $\hat{\Omega}$ using Eqs. (B5) and (B7):

$$dV = \sum_{m=0}^{d}\frac{1}{m!(d-m)!}\hat{c}_1^m \wedge \frac{\hat{\omega}_0^{d-m}}{(2\pi)^{d-m}}. \tag{B10}$$

APPENDIX C: CHARGE DENSITY FROM A GRADIENT EXPANSION IN THE QUANTUM MECHANICAL SYSTEM

In this Appendix, we demonstrate that the results for the charge density obtained from the semiclassical arguments in the main text can be confirmed by using a gradient expansion in the quantum mechanical system. We show that in metals the semiclassical formulas (3) and (4) are correct to first order in the spatial gradients. In insulators, the charge density vanishes

to first order in the spatial gradients, but the second-order term of Eq. (4) leads to the correct (quantized) total charge per skyrmion.

1. Gradient expansion of the Green's function

We follow the notation used in Ref. 47. For a spatially inhomogeneous system with Green's function $G(\omega;\mathbf{r}_1,\mathbf{r}_2)$, we introduce the Wigner transform of the Green's function

$$\tilde{G}(\omega;\mathbf{x}) \equiv \tilde{G}(\omega;\mathbf{R},\mathbf{k}) = \int d^3r\, e^{-i\mathbf{k}\cdot\mathbf{r}} G\left(\omega;\mathbf{R}+\frac{\mathbf{r}}{2},\mathbf{R}-\frac{\mathbf{r}}{2}\right), \quad \text{(C1)}$$

where $\mathbf{R}=\frac{1}{2}(\mathbf{r}_1+\mathbf{r}_2)$ and $\mathbf{r}=\mathbf{r}_1-\mathbf{r}_2$ are the center-of-mass and relative coordinates, respectively. The inverse K of the Green's function is defined by $\int d^3r' G(\omega;\mathbf{r}_1,\mathbf{r}')K(\omega;\mathbf{r}',\mathbf{r}_2) = \delta(\mathbf{r}_1-\mathbf{r}_2)$. In the Wigner representation, this relation becomes[47]

$$e^{\frac{i}{2}J_{ij}\partial_i^K\partial_j^G}\tilde{K}(\omega;\mathbf{x})\tilde{G}(\omega;\mathbf{x}) = \mathbb{1}, \quad \text{(C2)}$$

where $J=\left(\begin{smallmatrix}0 & \mathbb{1}\\ -\mathbb{1} & 0\end{smallmatrix}\right)$, the derivative ∂_i^K (∂_j^G) acts on $\tilde{K}$ ($\tilde{G}$) only, and the symbol $\mathbb{1}$ on the right-hand side of Eq. (C2) is the unit matrix in band space. For a smooth spatial variation, one can expand the exponential in Eq. (C2) in powers of spatial derivatives and solve order by order for $\tilde{G}$. We write

$$\tilde{G} \approx \tilde{G}_0 + \tilde{G}_1 + \tilde{G}_2 + \mathcal{O}\left(\partial_{R_i}^3\right), \quad \text{(C3)}$$

where the subscript indicates the order of spatial derivatives. Here, we truncate the gradient expansion after the second order to capture only the leading-order contribution to the charge density, which turns out to be linear in spatial gradients for metals and quadratic for insulators (see following).

The zero-order contribution $\tilde{G}_0$ is given by the pointwise inverse of $\tilde{K}$, i.e., $\tilde{G}_0(\omega,\mathbf{x}) = [\tilde{K}(\omega,\mathbf{x})]^{-1}$. In the limit of a homogeneous system, spatial gradients vanish and $\tilde{G} = \tilde{G}_0$. For a noninteracting homogeneous system $\tilde{K}(\omega,\mathbf{x}) \equiv \tilde{K}(\omega,\mathbf{k}) = \hbar\omega - H(\mathbf{k})$ where $H(\mathbf{k})$ is the band Hamiltonian.

If the system varies smoothly in space gradient corrections to the Green's function arise. The part of Eq. (C2) linear in spatial gradients reads as

$$\tilde{K}\tilde{G}_1 + \frac{i}{2}J_{ij}(\partial_i\tilde{K})(\partial_j\tilde{G}_0) = 0, \quad \text{(C4)}$$

where we omitted the dependency on ω and $\mathbf{x}$ to improve readability. With $\tilde{K} = \tilde{G}_0^{-1}$ follows

$$\tilde{G}_1 = \frac{i}{2}J_{ij}\tilde{G}_0\left(-\partial_i\tilde{G}_0^{-1}\right)\tilde{G}_0\left(-\partial_j\tilde{G}_0^{-1}\right)\tilde{G}_0 \equiv \quad \text{(C5)}$$

The last equality of Eq. (C5) introduces a graphical shorthand notation where a solid line represents $\tilde{G}_0$, a vertex labeled with i represents $(-\partial_i\tilde{G}_0^{-1})$ (where a minus sign is included in anticipation of the structure of higher-order terms) and a dashed arrow from a vertex i to a vertex j represents a factor of $\frac{i}{2}J_{ij}$.

The second-order part of Eq. (C2) reads as

$$\tilde{K}\tilde{G}_2 + \frac{i}{2}J_{ij}(\partial_i\tilde{K})(\partial_j\tilde{G}_1) + \frac{1}{2}\left(\frac{i}{2}\right)^2 J_{ij}J_{kl}(\partial_i\partial_k\tilde{K})(\partial_j\partial_l\tilde{G}_0) = 0. \quad \text{(C6)}$$

Solving Eq. (C6) for $\tilde{G}_2$ we arrive at [using the graphical notation introduced in Eq. (C5)]

$\tilde{G}_2 =$ 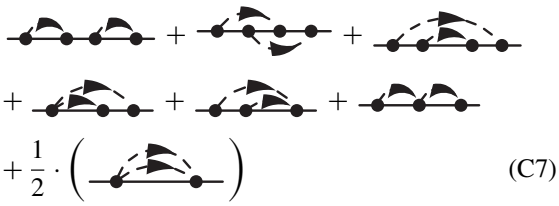 (C7)

where, e.g., the fourth diagram represents the term $(\frac{i}{2})^2 J_{ij}J_{kl}\tilde{G}_0(-\partial_i\partial_k\tilde{G}_0^{-1})\tilde{G}_0(-\partial_j\tilde{G}_0^{-1})\tilde{G}_0(-\partial_l\tilde{G}_0^{-1})\tilde{G}_0$.

2. Charge density in metals

The charge density is obtained from

$$\rho(\mathbf{R}) = e\frac{1}{\beta}\sum_{\omega_n}\int\frac{d^3k}{(2\pi)^3}\,\mathrm{Tr}[\tilde{G}(i\omega_n;\mathbf{R},\mathbf{k})], \quad \text{(C8)}$$

where $\tilde{G}$ is the Green's function in Wigner representation as defined in Eq. (C1), e is the electron charge, $\beta = 1/(k_BT)$ the inverse temperature, and $\hbar\omega_n = \frac{2\pi}{\beta}(n+\frac{1}{2})$. We use the gradient expansion Eq. (C3) for $\tilde{G}$. As $\tilde{G}_0(i\omega_n;\mathbf{R},\mathbf{k}) = 1/[i\hbar\omega_n - H(\mathbf{R},\mathbf{k})]$, the zero-order charge density $\rho^{(0)}(\mathbf{R})$ depends only on the local properties of the system at the point $\mathbf{R}$ and it is the same as the charge density of a homogeneous system described by the band Hamiltonian $H(\mathbf{R},\mathbf{k})$ at fixed $\mathbf{R}$.

In metals, the leading-order correction $\delta\rho^{(1)}(\mathbf{R})$ to the charge density is obtained by inserting $\tilde{G}_1$ from Eq. (C5) for $\tilde{G}$ into Eq. (C8). Standard techniques for the evaluation of Matsubara summations lead to

$$\delta\rho^{(1)}(\mathbf{R}) = -e\frac{i}{2}J_{ij}\int\frac{d^3k}{(2\pi)^3}\int_{-\infty}^{\infty}\frac{d\epsilon}{2\pi i}f(\epsilon) \times \mathrm{Tr}\left[\tilde{G}_0^R\left(-\partial_i\tilde{G}_0^{-1}\right)\tilde{G}_0^R\left(-\partial_j\tilde{G}_0^{-1}\right)\tilde{G}_0^R - \tilde{G}_0^A\left(-\partial_i\tilde{G}_0^{-1}\right)\tilde{G}_0^A\left(-\partial_j\tilde{G}_0^{-1}\right)\tilde{G}_0^A\right], \quad \text{(C9)}$$

where $f(\epsilon)$ is the Fermi function and $G^{R/A}$ is the retarded (advanced) Green's function, i.e., evaluated at frequencies $\epsilon/\hbar \pm i0^+$ just above (below) the real axis. We use the cyclicity of the trace and the relations $2i\,\mathrm{Im}\tilde{G} = \tilde{G}^R - \tilde{G}^A$ and $\partial\tilde{G}^{R/A}/\partial\epsilon = -(\tilde{G}^{R/A})^2$ to rewrite Eq. (C9):

$$\delta\rho^{(1)}(\mathbf{R}) = -ieJ_{ij}\int\frac{d^3k}{(2\pi)^3}\int_{-\infty}^{\infty}\frac{d\epsilon}{2\pi}f(\epsilon) \times \mathrm{Tr}\left[(\tilde{G}^A)^2\left(-\partial_i\tilde{G}_0^{-1}\right)\mathrm{Im}\tilde{G}\left(-\partial_j\tilde{G}_0^{-1}\right) - \frac{\partial\mathrm{Im}\tilde{G}}{\partial\epsilon}\left(-\partial_i\tilde{G}_0^{-1}\right)\tilde{G}_0^R\left(-\partial_j\tilde{G}_0^{-1}\right)\right]. \quad \text{(C10)}$$

Integrating by parts over ϵ in the second term in the trace and using the antisymmetry of J_{ij} leads to

$$\begin{aligned}\delta\rho^{(1)}(\mathbf{R}) &= -ieJ_{ij}\int\frac{d^3k}{(2\pi)^3}\int_{-\infty}^{\infty}\frac{d\epsilon}{2\pi}\Big(-f(\epsilon)\mathrm{Tr}\big[\mathrm{Im}\tilde{G}\,\big(-\partial_i\tilde{G}_0^{-1}\big)\\ &\quad\times\big(\big(\tilde{G}_0^R\big)^2+\big(\tilde{G}_0^A\big)^2\big)\big(-\partial_j\tilde{G}_0^{-1}\big)\big]+\frac{\partial f(\epsilon)}{\partial\epsilon}\\ &\quad\times\mathrm{Tr}\big[\mathrm{Im}\tilde{G}\,\big(-\partial_i\tilde{G}_0^{-1}\big)\tilde{G}_0^R\big(-\partial_j\tilde{G}_0^{-1}\big)\big]\Big).\end{aligned}\tag{C11}$$

In a noninteracting system $\tilde{G}_0^{R/A}(\omega;\mathbf{x})=[\hbar\omega-H(\mathbf{x})\pm i0^+]^{-1}$ and $\mathrm{Im}\tilde{G}(\omega;\mathbf{x})=-\pi\delta[\hbar\omega-H(\mathbf{x})]$. Direct evaluation of the two traces in Eq. (C11) in the local eigenbasis of $H(\mathbf{x})$ confirms the semiclassical result (12) where $\Omega_{n,ij}$ and $\delta\epsilon_n$ are given in Eqs. (7) and (8).

For the noninteracting system, the semiclassical approach is therefore exact to leading order in the spatial gradients. This is not the case when higher orders are considered. Already, the next higher-order contribution to the semiclassical charge density [coming from terms of order $\mathcal{O}(\Omega^2)$ in Eq. (4)] does not coincide with the higher-order terms of the gradient expansion [obtained by inserting $\tilde{G}_2$ into Eq. (C8)]. This is obvious from the appearance of second-order derivatives (i.e., vertices with two attached dashed arrows) on the right-hand side of Eq. (C7), which have no semiclassical counterpart.

The free energy can be calculated in a similar way by inserting the gradient expansion (C3) into $F=-T\sum_{\omega_n}\mathrm{Tr}\,\ln[-T\tilde{G}]$. The result confirms Eq. (6) to first order.

3. Quantized skyrmion charge in insulators

In insulators, as argued in the main text, the first-order correction to the charge density $\delta\rho^{(1)}(\mathbf{R})$ does not contribute to the total charge of a skyrmion. The leading-order contribution to the skyrmion charge in insulators is second order in spatial derivatives. In this section, we present the derivation of Eq. (14) using the gradient expansion method and give an explicit definition of the non-Abelian Berry curvature tensor. The derivation is similar to the calculation in Ref. 32, Appendix 2.

In a metal, $\tilde{G}(\omega)$ is analytical at $\omega=0$ and therefore Eq. (C8) simplifies (at $T=0$) to

$$\rho(\mathbf{R})=e\hbar\int\frac{d^3k}{(2\pi)^3}\int_{-\infty}^{\infty}\frac{d\omega}{2\pi}\,\mathrm{Tr}[\tilde{G}(i\omega;\mathbf{R},\mathbf{k})].\tag{C12}$$

The second-order correction to the charge density is given by inserting $\tilde{G}_2$ from Eq. (C7) into (C8). The contribution from the last term in Eq. (C7) is proportional to

$$\begin{aligned}&\hbar J_{ij}J_{kl}\int\frac{d\omega}{2\pi}\,\mathrm{Tr}\big[\tilde{G}_0\big(-\partial_i\partial_k\tilde{G}_0^{-1}\big)\tilde{G}_0\big(-\partial_j\partial_l\tilde{G}_0^{-1}\big)\tilde{G}_0\big]\\ &=-J_{ij}J_{kl}\int\frac{d\omega}{2\pi}\,\mathrm{Tr}\Big[\big(-\partial_i\partial_k\tilde{G}_0^{-1}\big)\tilde{G}_0\big(-\partial_j\partial_l\tilde{G}_0^{-1}\big)\frac{\partial\tilde{G}_0}{\partial\omega}\Big]\\ &=J_{ij}J_{kl}\int\frac{d\omega}{2\pi}\,\mathrm{Tr}\Big[\big(-\partial_i\partial_k\tilde{G}_0^{-1}\big)\frac{\partial\tilde{G}_0}{\partial\omega}\big(-\partial_j\partial_l\tilde{G}_0^{-1}\big)\tilde{G}_0\Big]\\ &=J_{ij}J_{kl}\int\frac{d\omega}{2\pi}\,\mathrm{Tr}\Big[\big(-\partial_j\partial_l\tilde{G}_0^{-1}\big)\tilde{G}_0\big(-\partial_i\partial_k\tilde{G}_0^{-1}\big)\frac{\partial\tilde{G}_0}{\partial\omega}\Big],\end{aligned}\tag{C13}$$

where all Green's functions are evaluated at frequency $i\omega$ and we used cyclicity of the trace in the first and the last equality, the relation $\partial\tilde{G}_0/\partial\omega=-\hbar(\tilde{G}_0)^2$ for a noninteracting system in the first equality, and integration by parts and the fact that $(\partial_i\tilde{G}_0^{-1})$ is independent of ω in the second equality. By relabeling indices and using $J_{ij}=-J_{ji}$ one sees that the last line of Eq. (C13) is the negative of the second line and hence vanishes. Thus, the last term in Eq. (C7) does not contribute to the charge density in insulators,

$\int\frac{d\omega}{2\pi}\,\mathrm{Tr}\Big[$  $\Big]=0.$ (C14)

In a similar way, one can show the relations

$\int\frac{d\omega}{2\pi}\,\mathrm{Tr}\Big[$  $\Big]=0$ (C15)

and

$\int\frac{d\omega}{2\pi}\,\mathrm{Tr}\Big[$ 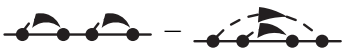 $\Big]=0.$ (C16)

Combining Eqs. (C12), (C7), and (C14)–(C16) leads to a simplified expression for the second-order correction to the charge density in insulators,

$\delta\rho^{(2)}(\mathbf{R})=e\hbar\int\frac{d^3k}{(2\pi)^3}\int\frac{d\omega}{2\pi}\,\mathrm{Tr}\Big[$ 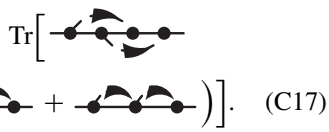 (C17)

To make further progress, we now focus on the contribution of $\delta\rho^{(2)}$ to the total charge of a skyrmion, given by $\delta Q^{(2)}=\int d^3R\,\delta\rho^{(2)}(\mathbf{R})$. The expression for $\delta Q^{(2)}$ can be simplified by means of integration by parts in phase space. The last diagram on the right-hand side of Eq. (C17) represents the term $(\frac{i}{2})^2J_{ij}J_{kl}\tilde{G}_0(-\partial_i\tilde{G}_0^{-1})\tilde{G}_0(-\partial_j\partial_k\tilde{G}_0^{-1})\tilde{G}_0(-\partial_l\tilde{G}_0^{-1})\tilde{G}_0$. It is structurally different from the other two diagrams in that it contains a second-order derivative in phase space. Integration by parts over the phase-space direction x_j or x_k, respectively, leads to the relations

$\int\frac{d^6x}{(2\pi)^3}$ 

$=-\int\frac{d^6x}{(2\pi)^3}\Big[$ 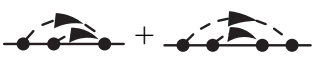

$=-\int\frac{d^6x}{(2\pi)^3}\Big[$ 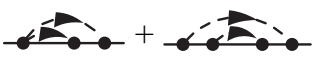 (C18)

Combining Eqs. (C15)–(C18) leads to

$\delta Q^{(2)}=\frac{e\hbar}{3}\int\frac{d^6x}{(2\pi)^3}\int\frac{d\omega}{2\pi}\,\mathrm{Tr}\Big[$ 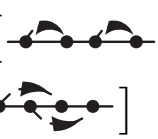

$=\frac{e\hbar}{3}\Big(\frac{i}{2}\Big)^2\int\frac{d^6x}{(2\pi)^3}\int\frac{d\omega}{2\pi}\,\mathcal{A}_{ijkl}\,\mathcal{B}_{ijkl}(i\omega,\mathbf{x})$ (C19)

with

$$\mathcal{A}_{ijkl} = J_{ij}J_{kl} + J_{il}J_{jk} - J_{ik}J_{jl} = -\epsilon_{ijkl},$$
$$\mathcal{B}_{ijkl}(i\omega,\mathbf{x}) = \mathrm{Tr}\big[\tilde{G}_0\big(-\partial_i\tilde{G}_0^{-1}\big)\tilde{G}_0\big(-\partial_j\tilde{G}_0^{-1}\big)\tilde{G}_0 \times\big(-\partial_k\tilde{G}_0^{-1}\big)\tilde{G}_0\big(-\partial_l\tilde{G}_0^{-1}\big)\tilde{G}_0\big]. \quad \text{(C20)}$$

The right-hand side of Eq. (C19) is the second Chern number, which is a topological invariant [cf., e.g., Eq. (53) in Ref. 33]. A similar calculation as in Appendix C of Ref. 33 leads to Eq. (14) where the (in general) non-Abelian Berry curvature Ω is now a matrix in the space of occupied bands with elements given by

$$\langle\mathbf{x},n|\Omega_{ij}|\mathbf{x},m\rangle = i\sum_{n'}\frac{\langle\mathbf{x},n|\frac{\partial H}{\partial x_i}|\mathbf{x},n'\rangle\langle\mathbf{x},n'|\frac{\partial H}{\partial x_j}|\mathbf{x},m\rangle - (i\leftrightarrow j)}{\big[\epsilon_n^{(0)}(\mathbf{x}) - \epsilon_{n'}^{(0)}(\mathbf{x})\big]\big[\epsilon_m^{(0)}(\mathbf{x}) - \epsilon_{n'}^{(0)}(\mathbf{x})\big]}, \quad \text{(C21)}$$

where $(i\leftrightarrow j)$ denotes the term with i and j exchanged.

4. Factorization of the skyrmion charge in insulators with Abelian Berry curvature

In this section, we show that the Berry curvature contribution to the charge in a two-dimensional insulator with Abelian Berry curvature is given by the product of the quantized Hall conductivity σ_{xy} and the skyrmion number Φ_0. An Abelian Berry curvature arises, e.g., if only a single band is occupied. We then derive an expression for the charge per length of a skyrmion line in a three-dimensional insulator.

For a two-dimensional system with only one occupied band, Eq. (14) reduces to

$$\delta Q^{(2)} = -\frac{e\,\epsilon_{ijkl}}{8}\int\frac{d^4x}{(2\pi)^2}\Omega_{ij}\Omega_{kl} = -\frac{e\,\epsilon_{ijkl}}{4}\left(\int\frac{dx_j\,dx_k\,dx_l}{(2\pi)^2}A_j\Omega_{kl}\right)_{x_i=-\infty}^{x_i=+\infty}, \quad \text{(C22)}$$

where the symbols $\pm\infty$ denote either positions far away from the skyrmion or the boundaries of the Brillouin zone for a space or momentum direction x_i, respectively. In the second equality of Eq. (C22), we used the relation

$$\frac{\epsilon_{ijkl}}{8}\Omega_{ij}\Omega_{kl} = \frac{\epsilon_{ijkl}}{2}\frac{\partial A_j}{\partial x_i}\frac{\partial A_l}{\partial x_k} = \frac{\epsilon_{ijkl}}{2}\frac{\partial}{\partial x_i}\left(A_j\frac{\partial A_l}{\partial x_k}\right) = \frac{\epsilon_{ijkl}}{4}\frac{\partial}{\partial x_i}(A_j\Omega_{kl}). \quad \text{(C23)}$$

In Eq. (C22), Ω_{kl} only enters at the boundary of the x_i coordinate. At the boundary in spatial direction (i.e., far away from the skyrmion), the magnetization is collinear and therefore $\Omega^{\mathrm{RR}} = 0 = \Omega^{\mathrm{Rk}}$. Thus, if x_i is a spatial coordinate, only terms of the form $A_j^{\mathrm{R}}\Omega_{kl}^{\mathrm{kk}}$ contribute to the integral kernel in Eq. (C22). If x_i is a momentum coordinate, Ω_{kl} is evaluated at the boundary of the Brillouin zone. In an insulator, the charge must be quantized and we can adiabatically deform the Bloch functions such that they are independent of momentum in a narrow stripe around the Brillouin zone boundary. This is always possible since, in the absence of further symmetries, all noninteracting Hamiltonians of one-dimensional insulators are adiabatically connected.[48] Therefore, only terms of the form $A_j^{\mathrm{k}}\Omega_{kl}^{\mathrm{RR}}$ contribute if x_i is a momentum coordinate. In total, Eq. (C22) can be written as $\delta Q^{(2)} = \delta Q^{(2),\mathrm{R}} + \delta Q^{(2),\mathrm{k}}$ where

$$\delta Q^{(2),\mathrm{R}} = -\frac{e\,\epsilon_{ij}}{2}\left(\int\frac{dR_j\,d^2k}{(2\pi)^2}A_j^R\Omega_{xy}^{kk}\right)_{R_i=-\infty}^{R_i=+\infty} \quad \text{(C24)}$$

and $\delta Q^{(2),\mathrm{k}}$ is defined by formally exchanging all R and k. As the Berry curvature $\Omega_{xy}^{\mathrm{kk}}$ in Eq. (C24) is gauge independent, it can not depend on R_j for a collinear magnetization at $R_i = \pm\infty$. This implies

$$\begin{aligned}\delta Q^{(2),\mathrm{R}} &= -\frac{e\,\epsilon_{ij}}{2}\int\frac{d^2k}{(2\pi)^2}\left(\Omega_{xy}^{\mathrm{kk}}\int dR_j\big(A_j^{\mathrm{R}}\big)_{R_i=-\infty}^{R_i=+\infty}\right)\\ &= -\frac{e}{2}\int\frac{d^2k}{(2\pi)^2}\left(\Omega_{xy}^{\mathrm{kk}}\int d^2R\,\epsilon_{ij}\frac{\partial A_j^{\mathrm{R}}}{\partial R_i}\right)\\ &= -\frac{e}{2}\int\frac{d^2k}{(2\pi)^2}\left(\Omega_{xy}^{\mathrm{kk}}\int d^2R\,\Omega_{xy}^{\mathrm{RR}}\right)\\ &= +\frac{1}{2}\sigma_{xy}\Phi_0, \end{aligned} \quad \text{(C25)}$$

where σ_{xy} (Φ_0) is the quantized integral over $\frac{e^2}{\hbar}\Omega_{xy}^{\mathrm{kk}}$ ($\frac{\hbar}{|e|}\Omega_{xy}^{\mathrm{RR}}$) as defined in the main text (recall that, in our convention, $e<0$ is the electron charge). An analogous calculation leads to the same value for $\delta Q^{(2),k}$. Thus, we conclude that the Berry curvature contribution to the skyrmion charge in a two-dimensional insulator with Abelian Berry curvature is given by

$$\delta Q^{(2)} = \sigma_{xy}\Phi_0. \quad \text{(C26)}$$

In three-dimensional systems, skyrmions form line defects. From Eqs. (B5) and (B7), the Berry curvature contribution to the charge in a three-dimensional insulator is given by

$$\delta Q^{(2)} = \frac{3e}{3!(2\pi)^3}\int\hat{\omega}_0\wedge\hat{\Omega}\wedge\hat{\Omega}. \quad \text{(C27)}$$

We introduce dimensionless coordinates $\tilde{\mathbf{x}} \equiv (\tilde{\mathbf{R}},\tilde{\mathbf{k}})$ such that $\mathbf{R} = \tilde{R}_\alpha\mathbf{a}_\alpha$ and $\mathbf{k} = \tilde{k}_\alpha\mathbf{g}_\alpha/(2\pi)$. Here, the vectors $\mathbf{a}_\alpha$ are lattice vectors of the atomic lattice and $\mathbf{g}_\alpha$ are the corresponding reciprocal lattice vectors. The coordinates $\tilde{\mathbf{x}}$ are chosen such that momentum space is periodic in the three coordinate directions $\tilde{k}_\alpha$ and the Jacobian of the transformation is one. In the dimensionless coordinates, Eq. (C27) reads as

$$\begin{aligned}\delta Q^{(2)} &= -\frac{e\,\epsilon_{\alpha\beta\gamma\delta\mu\nu}}{16}\int\frac{d^6\tilde{x}}{(2\pi)^3}J_{\alpha\beta}\tilde{\Omega}_{\gamma\delta}\tilde{\Omega}_{\mu\nu}\\ &= -e\sum_{\alpha=1}^{3}\int d\tilde{R}_\alpha\int\frac{d\tilde{k}_\alpha}{2\pi}\frac{\epsilon_{\alpha(\alpha+3)\gamma\delta\mu\nu}}{8}\int\frac{d^4\tilde{x}}{(2\pi)^2}\tilde{\Omega}_{\gamma\delta}\tilde{\Omega}_{\mu\nu}\\ &= -e\sum_{\alpha=1}^{3}\int d\tilde{R}_\alpha\int\frac{d\tilde{k}_\alpha}{2\pi}n_\alpha^{\mathrm{R}}n_\alpha^{\mathrm{k}}\end{aligned} \quad \text{(C28)}$$

with

$$n_\alpha^{\mathrm{R}} = \frac{\epsilon_{\alpha\gamma\delta}}{2} \int d\tilde{R}_\gamma d\tilde{R}_\delta \, \tilde{\Omega}^{\mathrm{RR}}_{\gamma\delta};$$
$$n_\alpha^{\mathrm{k}} = \frac{\epsilon_{\alpha\mu\nu}}{2} \int \frac{d\tilde{k}_\mu d\tilde{k}_\nu}{(2\pi)^2} \, \tilde{\Omega}^{\mathrm{kk}}_{\mu\nu}. \tag{C29}$$

In the first line of Eq. (C28), $\tilde{\Omega}_{\gamma\delta}$ denotes the elements of the Berry-curvature tensor in coordinates $\tilde{\mathbf{x}}$. The components of the symplectic tensor $J_{\alpha\beta}$ are invariant under the transformation from coordinates $\mathbf{x}$ to $\tilde{\mathbf{x}}$ due to the relation $\mathbf{a}_\alpha \cdot \mathbf{g}_\beta = 2\pi\delta_{\alpha\beta}$. This allowed us to set $\beta = \alpha + 3$ in the second line of Eq. (C28). The last integral in the second line of Eq. (C28) runs over the four-dimensional subspace of phase space perpendicular to $(\mathbf{0}, \mathbf{a}_\alpha)$ and $(\mathbf{g}_\alpha, \mathbf{0})$. Its value is given by the product of the real-space and the momentum-space winding numbers n_α^{R} and n_α^{k} by the same arguments that lead from Eq. (C22) to (C26).

The remaining integral over $\tilde{k}_\alpha$ in Eq. (C28) equates to a factor of 1 and the integral over $\tilde{R}_\alpha$ gives

$$\int d\tilde{R}_\alpha = \frac{\partial \tilde{R}_\alpha}{\partial R_i} \int dR_i = \frac{(\mathbf{g}_\alpha)_i}{2\pi} L_i = \frac{\hat{\mathbf{s}} \cdot \mathbf{g}_\alpha}{2\pi} L, \tag{C30}$$

where the unit vector $\hat{\mathbf{s}}$ points along along the skyrmion line and $L_i = L\hat{s}_i$ is the projection of the length L of the skyrmion line onto the coordinate direction R_i. For a generic skyrmion line that pierces all three position-space coordinate planes, the skyrmion number is $n_\alpha^{\mathrm{R}} = 1$ for all α. Combining Eqs. (C28) and (C30), we thus arrive at an expression for the charge per length of a skyrmion line in a three-dimensional insulator with Abelian Berry curvature

$$\frac{\delta Q^{(2)}}{L} = -e \sum_{\alpha=1}^{3} \frac{\hat{\mathbf{s}} \cdot \mathbf{g}_\alpha}{2\pi} n_\alpha^{\mathrm{k}}, \tag{C31}$$

where $\hat{\mathbf{s}}$ is the direction of the skyrmion line, $\mathbf{g}_\alpha$ are reciprocal lattice vectors, and $n_\alpha^{\mathrm{k}} \in \mathbb{Z}$ is defined in Eq. (C29).

*f.freimuth@fz-juelich.de

[1] I. Dzyaloshinsky, J. Phys. Chem. Solids **4**, 241 (1958).
[2] T. Moriya, Phys. Rev. **120**, 91 (1960).
[3] S. Mühlbauer, B. Binz, F. Jonietz, C. Pfleiderer, A. Rosch, A. Neubauer, R. Georgii, and P. Böni, Science **323**, 915 (2009).
[4] X. Z. Yu, Y. Onose, N. Kanazawa, J. H. Park, J. H. Han, Y. Matsui, N. Nagaosa, and Y. Tokura, Nature(London) **465**, 901 (2010).
[5] T. Schulz, R. Ritz, A. Bauer, M. Halder, M. Wagner, C. Franz, C. Pfleiderer, K. Everschor, M. Garst, and A. Rosch, Nat. Phys. **8**, 301 (2012).
[6] K. Everschor, M. Garst, B. Binz, F. Jonietz, S. Mühlbauer, C. Pfleiderer, and A. Rosch, Phys. Rev. B **86**, 054432 (2012).
[7] X. Z. Yu, N. Kanazawa, W. Z. Zhang, T. Nagai, T. Hara, K. Kimoto, Y. Matsui, Y. Onose, and Y. Tokura, Nat. Commun. **3**, 988 (2012).
[8] S. E. Barrett, G. Dabbagh, L. N. Pfeiffer, K. W. West, and R. Tycko, Phys. Rev. Lett. **74**, 5112 (1995).
[9] H. A. Fertig, L. Brey, R. Cote, and A. H. MacDonald, Phys. Rev. B **50**, 11018 (1994).
[10] S. L. Sondhi, A. Karlhede, S. A. Kivelson, and E. H. Rezayi, Phys. Rev. B **47**, 16419 (1993).
[11] D.-H. Lee and C. L. Kane, Phys. Rev. Lett. **64**, 1313 (1990).
[12] L. Brey, H. A. Fertig, R. Cote, and A. H. MacDonald, Phys. Rev. Lett. **75**, 2562 (1995).
[13] M. V. Berry, Proc. R. Soc. London, Ser. A **392**, 45 (1984).
[14] G. Sundaram and Q. Niu, Phys. Rev. B **59**, 14915 (1999).
[15] D. Xiao, M.-C. Chang, and Q. Niu, Rev. Mod. Phys. **82**, 1959 (2010).
[16] N. Nagaosa, J. Sinova, S. Onoda, A. H. MacDonald, and N. P. Ong, Rev. Mod. Phys. **82**, 1539 (2010).
[17] M. Lee, Y. Onose, Y. Tokura, and N. P. Ong, Phys. Rev. B **75**, 172403 (2007).
[18] Y. Yao, L. Kleinman, A. H. MacDonald, J. Sinova, T. Jungwirth, D.-s. Wang, E. Wang, and Q. Niu, Phys. Rev. Lett. **92**, 037204 (2004).
[19] X. Wang, J. R. Yates, I. Souza, and D. Vanderbilt, Phys. Rev. B **74**, 195118 (2006).
[20] S. Lowitzer, D. Ködderitzsch, and H. Ebert, Phys. Rev. Lett. **105**, 266604 (2010).
[21] J. Weischenberg, F. Freimuth, J. Sinova, S. Blügel, and Y. Mokrousov, Phys. Rev. Lett. **107**, 106601 (2011).
[22] I. Turek, J. Kudrnovský, and V. Drchal, Phys. Rev. B **86**, 014405 (2012).
[23] A. Neubauer, C. Pfleiderer, B. Binz, A. Rosch, R. Ritz, P. G. Niklowitz, and P. Böni, Phys. Rev. Lett. **102**, 186602 (2009).
[24] N. Kanazawa, Y. Onose, T. Arima, D. Okuyama, K. Ohoyama, S. Wakimoto, K. Kakurai, S. Ishiwata, and Y. Tokura, Phys. Rev. Lett. **106**, 156603 (2011).
[25] S. X. Huang and C. L. Chien, Phys. Rev. Lett. **108**, 267201 (2012).
[26] R. Cheng and Q. Niu, Phys. Rev. B **86**, 245118 (2012).
[27] F. Freimuth, S. Blügel, and Y. Mokrousov, arXiv:1308.5983.
[28] D. Xiao, J. Shi, and Q. Niu, Phys. Rev. Lett. **95**, 137204 (2005).
[29] P. J. Morrison, Rev. Mod. Phys. **70**, 467 (1998).
[30] A. Liechtenstein, M. Katsnelson, V. Antropov, and V. Gubanov, J. Magn. Magn. Mater. **67**, 65 (1987).
[31] F. Freimuth, S. Blügel, and Y. Mokrousov, arXiv:1305.4873.
[32] B.-J. Yang and N. Nagaosa, Phys. Rev. B **84**, 245123 (2011).
[33] X.-L. Qi, T. L. Hughes, and S.-C. Zhang, Phys. Rev. B **78**, 195424 (2008).
[34] T. Adams, S. Mühlbauer, C. Pfleiderer, F. Jonietz, A. Bauer, A. Neubauer, R. Georgii, P. Böni, U. Keiderling, K. Everschor, M. Garst, and A. Rosch, Phys. Rev. Lett. **107**, 217206 (2011).
[35] A. A. Mostofi, J. R. Yates, Y.-S. Lee, I. Souza, D. Vanderbilt, and N. Marzari, Comput. Phys. Commun. **178**, 685 (2008).
[36] F. Freimuth, Y. Mokrousov, D. Wortmann, S. Heinze, and S. Blügel, Phys. Rev. B **78**, 035120 (2008).
[37] Y. Ishikawa, G. Shirane, J. A. Tarvin, and M. Kohgi, Phys. Rev. B **16**, 4956 (1977).
[38] See http://www.flapw.de
[39] V. L. Moruzzi, J. F. Janak, and A. R. Williams, *Calculated Electronic Properties of Metals* (Pergamon, New York, 1978).
[40] T. Jeong and W. E. Pickett, Phys. Rev. B **70**, 075114 (2004).
[41] A. A. Mostofi *et al.*, Comput. Phys. Commun. **178**, 685 (2008).
[42] J. R. Yates, X. Wang, D. Vanderbilt, and I. Souza, Phys. Rev. B **75**, 195121 (2007).
[43] N. Marzari, A. A. Mostofi, J. R. Yates, I. Souza, and D. Vanderbilt, Rev. Mod. Phys. **84**, 1419 (2012).

[44]F. W. Warner, *Foundations of Differentiable Manifolds and Lie Groups* (Springer, New York, 1971).

[45]M. Göckeler and T. Schücker, *Differential Geometry, Gauge Theories, and Gravity* (Cambridge University Press, Cambridge, UK, 1989).

[46]J. Milnor and J. D. Stasheff, *Characteristic Classes*. (Princeton University Press, Princeton, NJ, 1974).

[47]J. Rammer and H. Smith, Rev. Mod. Phys. **58**, 323 (1986).

[48]S. Ryu, A. P. Schnyder, A. Furusaki, and A. W. W. Ludwig, New J. Phys. **12**, 065010 (2010).